PCCP

Accepted Manuscript

ROYAL SOCIETY OF CHEMISTRY

www.rsc.org/pccp

Journal Name

ARTICLE TYPE

Cite this: DOI: 10.1039/xxxxxxxxxx

Discrete variable representation of Smoluchowski equation using a sinc basis set

Andrea Piserchia* and Vincenzo Barone

Received Date
Accepted Date

DOI: 10.1039/xxxxxxxxxx

www.rsc.org/journalname

We present a new general framework for solving the monodimensional Smoluchowski equation using a discrete variable representation (DVR) based on the so called sinc basis set. The reliability of our implementation is assessed by comparing the convergence of diffusive operator eigenvalues calculated with our method and with a simple finite difference scheme for some model diffusive problems. The results here presented open encouraging possibilities for dealing with more complicated systems, where additional coordinate dependent terms in the equation or multidimensional treatments are needed and traditional methods often become unfeasible.

1 Introduction

The diffusion description of stochastic processes via the Smoluchowski equation has found widespread application in chemistry, in particular to describe kinetic processes that are diffusive in nature where fluctuations play an important role, and proper probabilistic modelization is needed[1]. This time-dependent partial derivative equation belongs to the wider class of Fokker-Planck equations that are used to model numerous systems in physics, chemistry, biology, finance and other research fields[2].

In particular, its mathematical structure is similar to Schrödinger's equation and this suggests analogous solution methods to solve it. The most common approaches in current use are finite-difference methods in space and time[3], and basis set expansions[4]. In the first kind of approaches one follows the evolution of the probability density $p(x,t)$ using finite difference approximations in x and t. On the other hand, the second class of methods is based on the projection of the time evolution operator upon a conventional basis of orthogonal functions, typically referred to as a spectral basis. Once constructed, the matrix representation of the operator is diagonalized in order to find the eigenvalues spectrum and then to calculate the time propagation.

A third class of methods that seems to straddle the boundary between grid discretization and basis function expansion are the so called pseudospectral methods which use functions that are localized on a grid in coordinate space. Among these methods, discrete variable representation (DVR) has enjoyed great success as highly accurate representation for the solution of a variety of problems in molecular vibration-rotation spectroscopy, reactive scattering, etc... [5–9] It's a well known numerical method within the quantum chemistry community for solving time-dependent Schrödinger's equation[10], while, to the best of our knowledge, this method has not yet seen widespread use in the "classical" community.

To construct a DVR, a finite basis of orthonormal functions, typically classical orthogonal polynomials or Fourier basis, is transformed to another orthonormal basis set (the DVR) in which each basis function is localized about one point of a coordinate space grid[11]. Those points are their associated grids of Gaussian quadrature points that, in the case of classical orthonormal polynomials, coincide with their roots. The advantages of using DVRs are the fact that they solve the problem of integral evaluation, because there are no integrals to evaluate, and the fact that they produce diagonal representations of coordinate functions (like the potential in Schrödinger's equation); while for derivative operators (such as kinetic energy) they usually produce analytical representations, depending on the starting basis set[5,12].

The real power of DVRs becomes evident in multidimensional problems, where the calculation of the operator's matrix representation is very cheap and for complicated operators, *i.e.* operators whose terms involve both (noncommuting) derivatives and functions of coordinate, where it is possible, in some instances, to use the product approximation[7,11].
This last aspect, as it will be pointed out in the next Section, is especially significant in connection with the Smoluchowski diffusion operator. In this first exploration we shall focus our attention on monodimensional problems of the general coordinate x, and we shall treat only bound potentials. DVR is used to approximate $p(x,t)$ and the time evolution operator, using a uniform grid in the coordinate x for which the corresponding basis set is a Fourier basis (also known as sinc methods).

The communication continues as follows: in Section "Theory" we provide both a rapid overview of the theory behind DVR of complicated operators, and the details on how to apply it to

Scuola Normale Superiore, piazza dei Cavalieri 7, I-56126 Pisa, Italy. Tel: +39 050 50 9347 E-mail: andrea.piserchia@sns.it

Smoluchowski equation; in Section "Case-study calculations" we show the application of the method to some specific familiar diffusion problems, and we make a comparison with another method, a simple finite difference (FD) scheme. After we have validated the new method we apply it to a chemical case-study represented by the diffusive torsion dynamic of some simple molecules. Finally, the Section "Conclusions" is dedicated to some discussion and perspectives. A short review of DVR theory is proposed in "Appendix A", and the FD scheme employed in this work is reported in "Appendix B".

2 Theory

2.1 DVR of complicated operators

DVR's are representations in bases of continuous functions which are in some sense localized "on a grid" in coordinate space. They are usually obtained by transformation from a truncated global basis, *i.e.* to construct a DVR, a finite basis of "global" orthonormal functions (typically orthogonal polynomials or Fourier basis) is transformed to another orthonormal basis set (the DVR) in which each basis function is "localized" about one point of a coordinate space grid $\{x_i\}$. The mathematical theory that underlies DVR and how they are constructed is well reported in the classical works of Light, Bačić and coworkers[11,13,14]. In order to not make heavier the reading, we have summarized this theory in Appendix A, where we address the interested Reader which might be unfamiliar with the general theory of DVR.

The essential feature of DVR is that we have a set of N basis functions $\{\theta_i(x)\}$ with the properties

$$\theta_i(x_j) = \sqrt{w'_j}\,\delta_{ij} \tag{1}$$

for a set of N points x_j and weights w'_j ($w'_j \equiv \sqrt{\frac{w(x_j)}{w_j}}$, cf. eqn (56) in Appendix A), and

$$\langle\theta_i|\theta_j\rangle = \int_a^b dx\,\theta_i(x)\,\theta_j(x) = \delta_{ij} \tag{2}$$

for an interval $[a,b]$ that contains all of the x_j.
DVRs are generally used with the approximation that the matrix representation of a general function of the coordinate is diagonal and the diagonal matrix elements are simply the values of the function at the DVR points (see eqn (57) in Appendix A).

For simple operators as $\frac{d^n}{dx^n}$, the DVR matrix $\mathbf{D}^{(n)\,\mathrm{DVR}}$ (with elements $D_{ij}^{(n)\,\mathrm{DVR}} = \langle\theta_i|\frac{d^n}{dx^n}|\theta_j\rangle$) is determined from transformation matrices and exact matrix representations of mono-dimensional operators in the original "delocalized" polynomial basis set. Of course, changing the global starting basis set (*e.g.* Legendre, Laguerre, Hermite polynomials, Fourier basis, etc...) will result in different $\mathbf{D}^{(n)\,\mathrm{DVR}}$. For $n = 1,2$ see refs.[5,12]. However, for complicated operators, *e.g.* $\Xi = \frac{d}{dx}F(x)\frac{d}{dx}$, with $F(x)$ a rational function, for which matrix elements of terms or factors with derivatives must be calculated numerically, defining a DVR is harder.

A DVR can be defined from a finite basis representation (FBR) where matrix elements of terms or factors in the complicated operator are computed by quadrature, but this step undermines the simplicity and convenience of the DVR. One may bypass quadrature by replacing the matrix representation of the whole operator with a product of matrix representations, making use of approximate resolution of the identity. This approach is usually referred to as *product approximation* and it reads:

$$\langle\theta_i|\Xi|\theta_j\rangle = \sum_{k,l=1}^{N} \langle\theta_i|\frac{d}{dx}|\theta_k\rangle\langle\theta_k|F(x)|\theta_l\rangle\langle\theta_l|\frac{d}{dx}|\theta_j\rangle \tag{3}$$

or in matrix form

$$\mathbf{\Xi}^{\mathrm{DVR}} = \mathbf{D}^{(1)\,\mathrm{DVR}}\,\mathbf{F}^{\mathrm{DVR}}\,\mathbf{D}^{(1)\,\mathrm{DVR}} \tag{4}$$

where $\mathbf{F}^{\mathrm{DVR}}$ is diagonal, $(\mathbf{F}^{\mathrm{DVR}})_{ij} = F(x_i)\,\delta_{ij}$. In some instances this approximation can spoil the Hermiticity of the operator; this will be seen in the next Section.

2.2 DVR applied to Smoluchowski equation

In the high-friction regime (also called overdamped regime) the Fokker-Planck equation simplifies into the Smoluchowski equation which, in one spatial dimension x, reads

$$\frac{\partial}{\partial t}\,p(x,t) = \frac{\partial}{\partial x}\,D(x)\,p_{eq}(x)\,\frac{\partial}{\partial x}\,p_{eq}^{-1}(x)\,p(x,t) \tag{5}$$

Here, $D(x)$ is a space-dependent diffusion coefficient and $p(x,t)$ is the probability density of finding a value of x at time t, with stationary limit $\lim_{t\to+\infty} p(x,t) = p_{eq}(x)$. In this case

$$p_{eq}(x) = \frac{e^{-\beta V(x)}}{Z} \tag{6}$$

is the canonical (Boltzmann) distribution, for the potential $V(x)$; with $\beta = 1/k_BT$ the Boltzmann factor and $Z = \int dx\,e^{-\beta V(x)}$ the partition function. Eqn (5) can be written as

$$\frac{\partial}{\partial t}\,p(x,t) = -\Gamma\,p(x,t) \tag{7}$$

where

$$\Gamma = -\frac{\partial}{\partial x}\,D(x)\,p_{eq}(x)\,\frac{\partial}{\partial x}\,p_{eq}^{-1}(x) \tag{8}$$

is the *diffusion operator*. In particular, in this work, we shall take in consideration only bound potentials, *i.e.* $V(x)$ goes to infinity at the endpoints of the domain, such that it's always possible to define $p_{eq}(x)$. Consequently we shall treat only cases with reflective or periodic boundary conditions.

The diffusion operator Γ is not Hermitian, so we will consider the symmetrized form of the operator. To this scope we multiply both members of eqn (7) by $p_{eq}^{-1/2}(x)$; defining $\widetilde{p}(x,t) = p_{eq}^{-1/2}(x)\,p(x,t)$

$$\frac{\partial}{\partial t}\,\widetilde{p}(x,t) = -\widetilde{\Gamma}\,\widetilde{p}(x,t) \tag{9}$$

and

$$\begin{aligned}\widetilde{\Gamma} &= p_{eq}^{-1/2}(x)\,\Gamma\,p_{eq}^{1/2}(x)\\ &= -p_{eq}^{-1/2}(x)\,\frac{\partial}{\partial x}\,D(x)\,p_{eq}(x)\,\frac{\partial}{\partial x}\,p_{eq}^{-1/2}(x)\end{aligned} \tag{10}$$

Now the eigenvalues $\{\lambda_i\}$ associated to this Hermitian operator are all real and the fact that diffusion $D(x)$ is a positive function,

assures that they are all positive. They regulate the time evolution of $p(x,t)$, describing the correct relaxation till the equilibrium state for a given initial distribution $p(x,0)$. In particular, the presence of a unique null eigenvalue $\lambda_0 = 0$ guarantees the existence of the equilibrium state while the positivity of the others guarantees to reach it; in fact λ_0 is associated to the eigenfunction $p_{eq}^{1/2}(x)$ since $\widetilde{\Gamma}\, p_{eq}^{1/2}(x) = 0$. The eigenvalues $\{\lambda_i\}$ have physical dimension of rates (inverse of time), and in the case of diffusive dynamics under the influence of a potential $V(x)$ that presents sufficiently deep wells separated by an energy gap, we can associate to small λ_i values "jump" processes between wells (*i.e.* slow activated processes where it is required to overpass the energy gap); high λ_i values can be associated, instead, to fluctuation processes inside the wells (fast processes). This aspect will be recalled in Section 3.2, when we treat the bistable potential.

At this point we can construct $\widetilde{\mathbf{\Gamma}}^{\mathrm{DVR}}$ matrix using an ordinary product approximation (as seen in Section 2.1); considering for brevity $M(x) = D(x)\, p_{eq}(x)$

$$\widetilde{\mathbf{\Gamma}}^{\mathrm{DVR}} = -\mathbf{P}_{eq}^{-1/2\,\mathrm{DVR}}\, \mathbf{D}^{(1)\,\mathrm{DVR}}\, \mathbf{M}^{\mathrm{DVR}}\, \mathbf{D}^{(1)\,\mathrm{DVR}}\, \mathbf{P}_{eq}^{-1/2\,\mathrm{DVR}} \tag{11}$$

As already mentioned, in some instances use of the product approximation can spoil the Hermiticity of the operator and of course, this problem may arise also in many dimensions. In this case we can see that depending on the chosen DVR basis functions, if $\mathbf{D}^{(1)\,\mathrm{DVR}}$ is not anti-Hermitian, $\widetilde{\mathbf{\Gamma}}^{\mathrm{DVR}}$ will not be Hermitian. In order to obtain an Hermitian DVR of the symmetrized diffusion operator by invoking the product approximation one must write $\widetilde{\mathbf{\Gamma}}^{\mathrm{DVR}}$ in the explicitly Hermitian form[7]

$$\check{\Gamma} = p_{eq}^{-1/2}(x) \left(\frac{\partial}{\partial x}\right)^{\dagger} M(x)\, \frac{\partial}{\partial x}\, p_{eq}^{-1/2}(x) \tag{12}$$

where $(\frac{\partial}{\partial x})^{\dagger} = \frac{\overleftarrow{\partial}}{\partial x}$ and the arrow denotes differentiation to the left. With this last expedient we have guaranteed Hermiticity to the operator, and in DVR it will be:

$$\check{\mathbf{\Gamma}}^{\mathrm{DVR}} = \mathbf{P}_{eq}^{-1/2\,\mathrm{DVR}}\, (\mathbf{D}^{(1)\,\mathrm{DVR}})^{\dagger}\, \mathbf{M}^{\mathrm{DVR}}\, \mathbf{D}^{(1)\,\mathrm{DVR}}\, \mathbf{P}_{eq}^{-1/2\,\mathrm{DVR}} \tag{13}$$

On the other hand, even if this procedure looks easy and straightforward, at the computational level it may cause some problems. In particular, when dealing with bound potentials (as in our case), the high values of $V(x)$ at the endpoints and inside the x domain (if present) generate numerical instability with great ease, due to the computation of $p_{eq}(x) \propto \exp(-\beta V(x))$. It is more convenient to consider the alternative form of the symmetrized operator

$$\widetilde{\Gamma} = -D(x)\left[\frac{\partial^2}{\partial x^2} + \frac{1}{2}\frac{\partial^2 V(x)}{\partial x^2} - \frac{1}{4}\left(\frac{\partial V(x)}{\partial x}\right)^2\right] - \frac{\partial D(x)}{\partial x}\frac{\partial}{\partial x} - \frac{1}{2}\frac{\partial D(x)}{\partial x}\frac{\partial V(x)}{\partial x} \tag{14}$$

obtained from eqn (10) using eqn (6) and setting out derivatives. Employing again the product approximation is straightforward, since the derivatives of the potential and diffusion are simple functions of x and consequently their DVR matrices are diagonal. One has only to carry about DVR of derivative operators terms, $\mathbf{D}^{(1)\,\mathrm{DVR}}$ and $\mathbf{D}^{(2)\,\mathrm{DVR}}$ in this case. The great advantage of using this way, instead of eqn (13), is that one can manage great values of $V(x)$ with no numerical problems, but the drawback is that both $\mathbf{D}^{(1)\,\mathrm{DVR}}$ and $\mathbf{D}^{(2)\,\mathrm{DVR}}$ must be Hermitian in order to have $\widetilde{\mathbf{\Gamma}}^{\mathrm{DVR}}$ to be Hermitian as well. This requirement is fulfilled using sinc-DVR (that is constructed in turn on Fourier basis, see Subsection "sinc-DVR" in Appendix A)[5,6], but not using other DVRs[12].

Following Colbert and Miller[5], we consider probability densities $p(x,t)$ that are defined on a grid consisting of $N-1$ equally spaced grid points $\{x_i\}$ on the range $[a,b]$

$$x_i = a + i\frac{(b-a)}{N}, \quad i = 1,\ldots,N-1 \tag{15}$$

In this case the weights coincide simply with $\Delta x = \frac{b-a}{N}$, the grid spacing and the corresponding DVR-functions are sinc functions

$$\theta_i(x) = \frac{1}{\sqrt{\Delta x}}\,\mathrm{sinc}\left[\frac{\pi(x-x_i)}{\Delta x}\right] = \sqrt{\Delta x}\,\frac{\sin(\pi(x-x_i)/\Delta x)}{\pi(x-x_i)} \tag{16}$$

These functions are "localized" on the grid points; indeed they are equal to $\frac{1}{\sqrt{\Delta x}}$ for $x = x_i$ and zero for $x = x_j$, $j \neq i$.
In the case of reflective boundary conditions the associated $N-1$ (FBR) functions for a uniform grid are the particle-in-a-box eigenfunctions

$$\phi_m(x) = \sqrt{\frac{2}{b-a}}\,\sin\left[\frac{m\pi(x-a)}{b-a}\right], \quad m = 1,\ldots,N-1 \tag{17}$$

where the range has to be taken in the mathematical limit $a \to -\infty, b \to +\infty, N \to +\infty$. The DVR elements of the two derivative operators are given by[5,6]

$$(\mathbf{D}^{(1)})_{ij} = \begin{cases} 0 & i = j \\ \frac{1}{\Delta x}\frac{(-1)^{i-j}}{i-j} & i \neq j \end{cases} \tag{18}$$

$$(\mathbf{D}^{(2)})_{ij} = \begin{cases} -\frac{1}{3}\frac{\pi^2}{\Delta x^2} & i = j \\ -\frac{2}{\Delta x^2}\frac{(-1)^{i-j}}{(i-j)^2} & i \neq j \end{cases} \tag{19}$$

On the other hand, in the case of periodic boundary conditions in the range $[0, 2\pi]$, the appropriate basis functions are

$$\phi_m(x) = \frac{e^{imx}}{\sqrt{2\pi}}, \quad m = 0, \pm1, \pm2, \ldots, \pm N \tag{20}$$

and the $2N+1$ grid points are

$$x_i = i\frac{2\pi}{2N+1}, \quad i = 1,\ldots,2N+1 \tag{21}$$

The most complicated step of this procedure is the evaluation of the first derivative operator. Although the matrix elements are readily derived and evaluated using procedures analogous to those presented by Colbert and Miller, to the best of our knowledge, they have not yet been reported. However, with similar derivations as in ref.[5]

$$(\mathbf{D}^{(1)})_{ij} = \begin{cases} 0 & i = j \\ \frac{1}{2N+1}\frac{\frac{1}{2}N\sin\frac{2\pi(N+1)(i+j)}{2N+1} - \frac{1}{2}(N+1)\sin\frac{2\pi N(i+j)}{2N+1}}{\sin^2\frac{\pi(i+j)}{2N+1}} & i \neq j \end{cases} \tag{22}$$

$$(\mathbf{D}^{(2)})_{ij} = \begin{cases} -\frac{N(N+1)}{3} & i = j \\ -\frac{(-1)^{i-j}\cos[\pi(i-j)/(2N+1)]}{2\sin^2[\pi(i-j)/(2N+1)]} & i \neq j \end{cases} \quad (23)$$

Using these expressions, once the bound potential $V(x)$ and the diffusion coefficient $D(x)$ are given, $\widetilde{\mathbf{\Gamma}}^{\mathrm{DVR}}$ is easily constructed using product approximation on eqn (14). Then, eigenvalues and eigenfunctions are calculated from the numerical diagonalization of $\widetilde{\mathbf{\Gamma}}^{\mathrm{DVR}}$. Given the initial distribution $p(x,0)$, the profile $p(x,t)$ is built expanding upon DVR functions calculated at DVR points $\{x_i\}$ for which θ_i's are equal to $\frac{1}{\sqrt{\Delta x}}$, cf. eqns (1,16).

3 Case-study calculations

In this Section, we apply the methodology sketched in the preceding section to some diffusive test problems described with Smoluchowski equation, considering different potentials and the effect of a constant or variable diffusion coefficient. Our objective is to determine the eigenvalues (λ^{DVR} in the following) of the DVR diffusion operator matrix $\widetilde{\mathbf{\Gamma}}^{\mathrm{DVR}}$, calculated using sinc-DVR with product approximation on eqn (14) as shown in the previous Section. In particular we shall focus on three different kinds of potentials, namely the analytic case of harmonic potential and the well known case of bistable potential with equivalent and nonequivalent minima that is usually adopted in the modelization of numerous chemical problems. In order to illustrate the validity of the method we concentrate on the eigenvalue convergence, *i.e.* how many grid points (N_{points} in the following) are necessary for sinc-DVR to provide accurate first eigenvalues in order to have a reliable description of the system. We compare them with analytic results (where possible) or with values calculated by other methods, in particular, a simple finite difference (FD) scheme (reported in Appendix B), λ^{FD} in the following. We remark that for reflective boundary conditions $N_{\mathrm{points}} \equiv N-1$ while for periodic ones $N_{\mathrm{points}} \equiv 2N+1$ (see Section 2.2); from now on the potential $V(x)$ is expressed in k_BT units.

3.1 Harmonic potential

It is always convenient to make reference to analytic cases when a new method is tested. One of these is the monodimensional diffusion problem over a parabolic potential, shown in Figure 1, with a constant diffusion coefficient $D(x) = D$, also known as Ornstein-Uhlenbeck process [15,16]

$$V(x) = \frac{1}{2}kx^2 \quad (24)$$

Here, x is defined over the entire real axis and k denotes the force constant; the axes origin is chosen such as to coincide with the potential minimum. Physically this case can be used to describe the local oscillatory dynamic of molecules in a certain phase (*e.g.* a liquid crystal that is fluctuating inside a smectic phase). Boundary conditions are reflective and eigenvalues are simply [17]

$$\lambda_m = mkD, \quad m = 0,1,2,\ldots \quad (25)$$

with the null eigenvalue λ_0 associated to the stationary solution

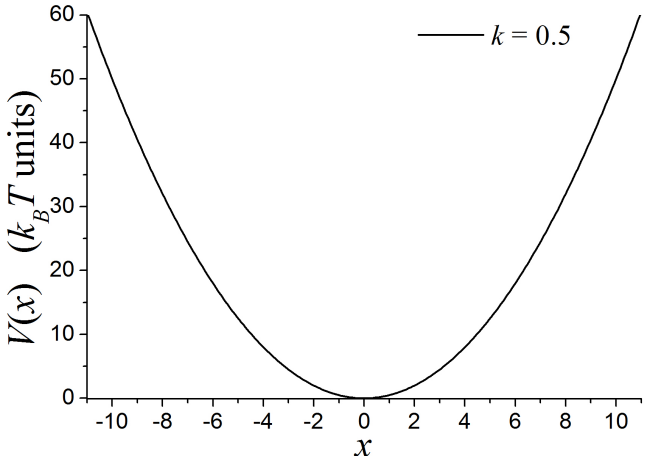

Fig. 1 Plot of the harmonic potential used in our calculations, eqn (24).

$$p_{eq}(x) = \frac{e^{-V(x)}}{\int_{-\infty}^{+\infty} dx\, e^{-V(x)}} = \sqrt{\frac{k}{2\pi}} e^{-\frac{kx^2}{2}} \quad (26)$$

The x range for calculations is chosen following the proposal of Colbert and Miller [5], that is, introducing an energy cutoff V_{cutoff} for the potential energy and discarding grid points for which:

$$V(x_i) > V_{\mathrm{cutoff}} \quad (27)$$

i.e. where the probability density $p(x,t)$ would be negligibly small. Practically, we accomplish this by choosing a range for which the gap: potential at the endpoints/potential at the global minima is less than 50 k_BT units. Convergence of the calculation can also be checked by increasing the energy cutoff, but for the sake of simplicity and since we have chosen a large enough V_{cutoff}, this will not be discussed.

In Table 1 we report the convergence of the first ten nonzero eigenvalues calculated with DVR method, given in diffusion coefficient units (that is equivalent to have taken $D = 1$, *i.e.* D is a scaling factor for the eigenvalues) and shown up to five significant figures, for $k = 1.0$ and x range $[-10.0, 10.0]$. We compare them with the ones calculated using the FD scheme. As it can be easily seen, the convergence is more rapid using DVR instead of FD; in particular for $N_{\mathrm{points}} > 26$ we are just at convergence, while for FD, more than 65 and more than 210 grid points are required in order to have respectively λ_1^{FD} and $\lambda_{10}^{\mathrm{FD}}$ converged up to five significant figures.

3.2 Bistable potential

Another suitable model to test the DVR method, is the well known bistable potential, that has the general shape sketched in Figure 2: two minima a and c respectively, separated by a potential maximum b and bound at the endpoints. There are several examples of bistable systems, those analyzed most often in the literature being the laser, the tunnel diode [18], and more generally activated reactions, *e.g.* hindered rotations.

As anticipated in Section 2.2, when the barrier that separates the two minima is sufficiently high, the diffusion process from a to c and vice versa is said to be activated. In this situation,

Table 1 Convergence of the first ten nonzero eigenvalues, given in diffusion coefficient units and shown up to five significant figures, for the harmonic potential, eqn (24), with $k = 1.0$ and x range $[-10.0, 10.0]$, calculated with DVR method and FD scheme, respectively, λ^{DVR} and λ^{FD}.

N_{points}	λ_1^{DVR}	λ_2^{DVR}	λ_3^{DVR}	λ_4^{DVR}	λ_5^{DVR}	λ_6^{DVR}	λ_7^{DVR}	λ_8^{DVR}	λ_9^{DVR}	$\lambda_{10}^{\mathrm{DVR}}$
6	0.63371	4.4689	4.5375	12.655	12.677					
8	0.76420	2.9013	3.0612	7.8742	7.9163	15.303	15.323			
10	0.92271	2.2799	2.6542	5.6605	5.7480	10.624	10.658	17.280	17.300	
12	0.98723	2.0638	2.7630	4.6092	4.8203	8.1653	8.2305	12.892	12.923	18.909
14	0.99876	2.0094	2.9385	4.1662	4.6719	6.8699	7.0204	10.406	10.463	14.835
16	0.99992	2.0008	2.9928	4.0288	4.8753	6.2616	6.6567	9.0108	9.1386	12.437
18	1.0000	2.0000	2.9995	4.0028	4.9829	6.0493	6.8302	8.3163	8.6640	11.037
20	1.0000	2.0000	3.0000	4.0002	4.9988	6.0051	6.9750	8.0608	8.8133	10.323
22	1.0000	2.0000	3.0000	4.0000	5.0000	6.0003	6.9983	8.0061	8.9731	10.060
24	1.0000	2.0000	3.0000	4.0000	5.0000	6.0000	6.9999	8.0003	8.9983	10.006
26	1.0000	2.0000	3.0000	4.0000	5.0000	6.0000	7.0000	8.0000	9.0000	10.000
28	1.0000	2.0000	3.0000	4.0000	5.0000	6.0000	7.0000	8.0000	9.0000	10.000
30[a]	1.0000	2.0000	3.0000	4.0000	5.0000	6.0000	7.0000	8.0000	9.0000	10.000

N_{points}	λ_1^{FD}	λ_2^{FD}	λ_3^{FD}	λ_4^{FD}	λ_5^{FD}	λ_6^{FD}	λ_7^{FD}	λ_8^{FD}	λ_9^{FD}	$\lambda_{10}^{\mathrm{FD}}$
6	0.72186	93.365	93.365	24150	24150					
8	0.69747	7.9693	7.9708	181.03	181.03	4120.2	4120.2			
10	0.80433	3.1002	3.1203	22.513	22.513	166.29	166.29	1228.7	1228.7	
12	0.91504	2.1594	2.2633	8.2333	8.2333	32.869	32.869	131.78	131.78	528.49
14	0.96955	1.9344	2.2284	4.9808	4.9821	13.544	13.544	37.479	37.479	103.94
16	0.98603	1.9112	2.4633	3.9550	3.9730	8.2174	8.2174	17.758	17.758	38.701
18	0.99180	1.9350	2.7130	3.6684	3.7885	6.2576	6.2581	11.289	11.289	20.764
20	0.99470	1.9569	2.8430	3.6731	4.0490	5.5100	5.5196	8.6252	8.6252	13.955
22	0.99640	1.9708	2.8989	3.7574	4.4227	5.3311	5.4241	7.4555	7.4561	10.880
24	0.99747	1.9796	2.9299	3.8302	4.6483	5.4200	5.7815	7.0293	7.0429	9.4068
26	0.99817	1.9852	2.9496	3.8786	4.7570	5.5702	6.2318	7.0302	7.1653	8.7705
28	0.99864	1.9891	2.9628	3.9108	4.8229	5.6873	6.4848	7.2247	7.6825	8.6494
30	0.99897	1.9917	2.9719	3.9328	4.8672	5.7670	6.6225	7.4226	8.1307	8.8386

[a] For $N_{\mathrm{points}} = 30$ convergence up to 5 significant figures is reached till λ_{15}.

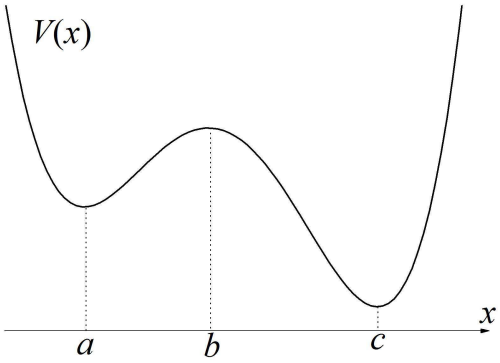

Fig. 2 Sketch of a generic bistable potential; b individuates the maximum that separates the two minima a, c.

the lowest nonzero eigenvalue λ_1 is associated with the "jump" process between the two wells and its value is generally separated by several orders of magnitude from the the others. When the barrier height increase, λ_1 gets smaller, showing an Arrhenius law behaviour, and in this limit it can be identified as[19]

$$\lambda_1 = r_{ac} + r_{ca} \tag{28}$$

where r_{ac} and r_{ca} are the escape rates from well a towards well c and vice versa. Kramers in his pioneering work[20] has shown that for the reaction dynamics in a bistable potential, with constant diffusion coefficient ($D(x) = D$), these rates can be approximated as

$$r_{ac}^{\mathrm{K}} = \frac{\sqrt{V^{(2)}(a)\,|V^{(2)}(b)|}}{2\pi}\, e^{-\frac{V(b)-V(a)}{D}} \tag{29}$$

where the vertical bars indicate the absolute value and $V^{(n)}$ indicates the nth-order derivative $\frac{d^n V(x)}{dx^n}$. To calculate r_{ca} one has simply to exchange a with c in the previous equation.

This asymptotic result has been refined many years later by Edholm and Leimar[21] who calculated an improved expression for the escape rate

$$r_{ac}^{\mathrm{E}} = r_{ac}^{\mathrm{K}}\left[1 - D\left(\frac{1}{8}\frac{V^{(4)}(b)}{[V^{(2)}(b)]^2} - \frac{1}{8}\frac{V^{(4)}(a)}{[V^{(2)}(a)]^2} + \frac{5}{24}\frac{[V^{(3)}(b)]^2}{|V^{(2)}(b)|^3} + \frac{5}{24}\frac{[V^{(3)}(a)]^2}{[V^{(2)}(a)]^3}\right) + O([V(b)-V(a)]^2)\right] \tag{30}$$

which gives a better approximation to eqn (29). This result is important for a first comparison between the calculated λ_1^{DVR} and λ_1^{FD}, for different functional forms of the bistable potential (see below), where analytic expressions are not available for the eigenvalues.

In the following we take in consideration the two different cases of symmetric and non-symmetric bistable potentials in order to provide a more complete picture; for the last case we discuss also the situation of a non-constant diffusion coefficient.

Symmetric case

A symmetric potential ($V(x) = V(-x)$) is characterized by equivalent minima $V(a) = V(c)$, and with a constant diffusion coefficient D we also have that $r_{ac} = r_{ca}$. By calling $V(b) - V(a) = V_0$ the energy barrier height, we take in consideration two different functional forms for $V(x)$, respectively

$$V(x) = V_0 \left(x^2 - 1\right)^2 \tag{31}$$

for which we apply reflective boundary conditions and

$$V(x) = \alpha \cos x + 2\alpha \cos 2x \tag{32}$$

for which we apply periodic boundary conditions. In the last equation α is a parameter and the energy barrier will be $V_0(\alpha)$. Just to mention, the potential in eqn (31) is also known as the quartic potential or "Landau-Ginzburg potential" and is a popular model for bistable systems[19]. On the other hand, the potential of eqn (32) can be used to describe the diffusive problem involving a torsional angle. The potentials and the parameters used in our calculations are reported in Figure 3 where the profiles are shifted to the origin in order to have a direct comparison of the barrier heights.

In Table 2 we report the convergence of the first three nonzero eigenvalues calculated with the DVR method, given in diffusion coefficient units and shown up to five significant figures, for different values of the barrier heights V_0, and $V_0(\alpha)$. We compare our results with those issuing from a FD calculation and with the λ_1's obtained with the Edholm's approximation

$$\lambda_1^{\mathrm{E}} = 2\, r_{ac}^{\mathrm{E}} \tag{33}$$

using eqn (30). We want to stress that eqns (28, 29, 30) are only good approximations to λ_1 and one should not take λ_1^{E} as the *true* value to be reached. Finally, for the periodic potential eqn (32) we also report the first three nonzero eigenvalues obtained using the orthonormal representation (OR) method with a Fourier basis, for which the matrix elements of the diffusion operator are analytical.

As anticipated above, λ_1's always differs by several orders of magnitude from λ_2's and λ_3's and this gap increases as V_0 becomes larger, implying different time scales for the diffusive relaxation processes.

Secondly, in all cases, λ_1's converge collectively to values slightly different from λ_1^{E}, confirming the fact that these last ones should not be taken as exact reference values. Finally, we see that for the two cases of lowest energy barriers, λ_1^{FD} converge up to five significant figures more slowly than λ_1^{DVR}, while the same cannot be said doubling V_0. However, in all instances, for the other two eigenvalues (λ_2, λ_3) FD shows a very slow convergence compared to DVR, and in order to have the first three nonzero eigenvalues all equal to DVR ones, up to the fifth significant figure, we have to use a huge number of grid points. Indeed, in order of potential appearance as in Table 2, we need respectively more than 450, 1500, 750 and 1500 grid points to reach convergence with FD to the same values calculated with DVR; which need fewer points. So, as an example, for the quartic potential with $V_0 = 10.0$ using

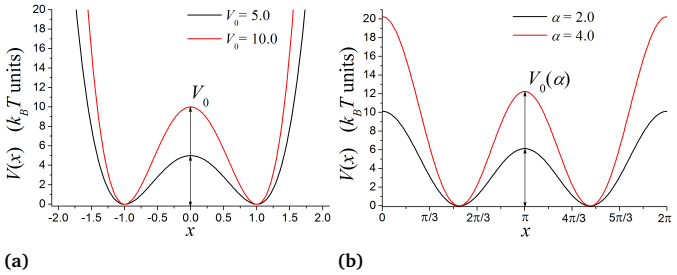

Fig. 3 Plot of the quartic potential, eqn (31) (panel a), and of the periodic potential, eqn (32) (panel b). Both profiles are shifted with respect to the origin in order to emphasize the energy barriers involved, V_0 and $V_0(\alpha)$ respectively.

FD we need 1500 grid points in order to have λ_i^{FD} $(i = 1,2,3)$ equal to the ones calculated with DVR; this shows the slow convergence of FD as opposed to DVR. These simple examples (together with the harmomic potential) show how DVR can be used to reproduce accurately the eigenvalue spectrum of the diffusion operator and consequently to describe the correct relaxation dynamics till the equilibrium with a low computational effort.

Non-symmetric case

Finally we consider a non-symmetric bistable potential with nonequivalent minima $V(a) \neq V(c)$, and with non-constant diffusion coefficient. In particular we analyze a periodic potential of the form

$$V(x) = \alpha_1 \cos x + 2\alpha_1 \cos 2x - \alpha_2 \sin x \tag{34}$$

with fixed parameters $\alpha_1 = 2.0$, $\alpha_2 = 1.5$, shown in Figure 4. This potential could describe the energetics of a torsional angle that identifies, for example, the relative orientation between two parts of a molecule and it has been shown how to compute well sound variable diffusion coefficients for this kind of situations[22]. Starting from constant diffusion coefficient, it is clear that a change in the coefficient would produce only a scaling of the eigenvalues (as stated previously); in particular, as D increases, the friction that damps the motion while keeping it alive at the same time[23] gets smaller, and the eigenvalues get increased accelerating the relaxation dynamics; of course, the opposite behaviour is observed when D decreases. However, when the diffusion coefficient is no longer constant, it is difficult to predict a priori its effect on the eigenvalues; to this purpose, here we treat four different cases

$$D(x) = \pm \cos x + c \tag{35}$$

and

$$D(x) = \pm \sin x + c \tag{36}$$

with fixed shift $c = 2.0$. These four functions are chosen in order to see the effect of locally increasing the diffusion around respectively the two endpoints and around the maximum, eqn (35); and respectively around the left and right minima of the potential, eqn (36).

In Table 3 we report the first three converged eigenvalues for the non-symmetric bistable potential eqn (34) with different diffusion coefficients eqns (35,36), calculated with the DVR method.

Table 2 Convergence of the first three nonzero eigenvalues, given in diffusion coefficient units and shown up to five significant figures, for the bistable potentials, eqns (31,32), for different values of V_0, and $V_0(\alpha)$, calculated with DVR method and FD scheme. Comparison is also shown for Edholm λ_1^{E}, calculated with eqn (33). The last entries for λ_i^{DVR} for each potential are the converged values, also reached by FD but using more points (see text).

N_{points}	λ_1^{DVR}	λ_1^{FD}	λ_1^{E}	λ_2^{DVR}	λ_2^{FD}	λ_3^{DVR}	λ_3^{FD}
$V_0 = 5.0$[a]			5.6113×10^{-2}				
20	7.9016×10^{-2}	5.5459×10^{-2}		16.448	16.462	26.287	25.943
25	5.5693×10^{-2}	5.5491×10^{-2}		16.445	16.460	26.282	26.082
30	5.5505×10^{-2}	5.5501×10^{-2}		16.445	16.457	26.283	26.146
35	5.5523×10^{-2}	5.5506×10^{-2}		16.445	16.454	26.283	26.184
40	5.5523×10^{-2}	5.5510×10^{-2}		16.445	16.452	26.283	26.208
$V_0 = 10.0$[a]			7.8683×10^{-4}				
35	4.8909×10^{-4}	7.8357×10^{-4}		36.170	36.325	58.181	59.439
40	7.7788×10^{-4}	7.8357×10^{-4}		36.170	36.297	58.181	59.165
45	7.8386×10^{-4}	7.8357×10^{-4}		36.170	36.275	58.181	58.970
50	7.8368×10^{-4}	7.8357×10^{-4}		36.170	36.257	58.181	58.826
55	7.8368×10^{-4}	7.8357×10^{-4}		36.170	36.244	58.181	58.717
$\alpha = 2.0$, $V_0 = 6.125$[b,c]			9.6862×10^{-3}				
21	1.1167×10^{-2}	9.6731×10^{-3}		10.426	10.624	12.867	12.952
25	9.7230×10^{-3}	9.6744×10^{-3}		10.426	10.572	12.871	12.940
31	9.6771×10^{-3}	9.6753×10^{-3}		10.426	10.524	12.871	12.922
35	9.6772×10^{-3}	9.6757×10^{-3}		10.426	10.504	12.871	12.913
41	9.6772×10^{-3}	9.6761×10^{-3}		10.426	10.484	12.871	12.903
$\alpha = 4.0$, $V_0 = 12.25$[b,d]			4.3806×10^{-5}				
35	4.8442×10^{-5}	4.3487×10^{-5}		25.244	25.418	28.800	28.938
41	4.3282×10^{-5}	4.3487×10^{-5}		25.244	25.393	28.800	28.931
45	4.3462×10^{-5}	4.3487×10^{-5}		25.244	25.376	28.800	28.920
51	4.3484×10^{-5}	4.3487×10^{-5}		25.244	25.353	28.800	28.903
55	4.3487×10^{-5}	4.3487×10^{-5}		25.244	25.341	28.800	28.892
61	4.3487×10^{-5}	4.3487×10^{-5}		25.244	25.341	28.800	28.892

[a] The selected x range is $[-2.0, 2.0]$.
[b] The selected x range is $[0, 2\pi]$.
[c] Using orthonormal representation method with a Fourier basis, at convergence: $\lambda_1^{\mathrm{OR}} = 9.6772\times10^{-3}, \lambda_2^{\mathrm{OR}} = 10.426, \lambda_3^{\mathrm{OR}} = 12.871$.
[d] Using orthonormal representation method with a Fourier basis, at convergence: $\lambda_1^{\mathrm{OR}} = 4.3487\times10^{-5}, \lambda_2^{\mathrm{OR}} = 25.244, \lambda_3^{\mathrm{OR}} = 28.800$.

Also FD converges to the same DVR values, but more slowly; indeed to reach convergence with constant diffusion (first entry in Table 3) we just need 35 grid points with DVR method, while more than 800 grid points are required using FD. In the case of variable diffusion function (last four entries in Table 3) we just need 45 grid points with DVR method, while more than 1300 grid points are required using FD to reach the same λ_i^{DVR} $(i=1,2,3)$.

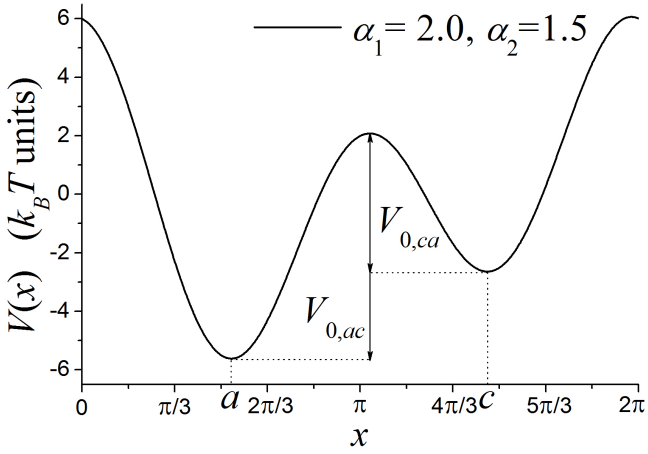

Fig. 4 Plot of the non-symmetric potential, eqn (34); a, c individuate the two minima separated by the energy barriers $V_{0,ac} = 7.4670$ and $V_{0,ca} = 4.3543\ k_BT$ units going respectively from a to c, and vice versa.

Table 3 First three converged eigenvalues calculated with DVR method and shown up to five significant figures, for the non-symmetric bistable potential eqn (34) with different diffusion functions eqns (35,36).

Diffusion function	λ_1^{DVR}	λ_2^{DVR}	λ_3^{DVR}
$D(x) = D^a$	1.9435×10^{-2}	9.8592	13.418
$D(x) = \cos x + 2.0$	2.1135×10^{-2}	12.467	20.132
$D(x) = -\cos x + 2.0$	5.6454×10^{-2}	17.145	23.545
$D(x) = \sin x + 2.0$	3.5715×10^{-2}	11.949	19.751
$D(x) = -\sin x + 2.0$	4.0402×10^{-2}	15.321	22.124

[a] For a constant diffusion, we can use eqns (28,30) to calculate estimated $r_{ac}^{\mathrm{E}} = 1.1381\times10^{-3}, r_{ca}^{\mathrm{E}} = 2.0473\times10^{-2}, \lambda_1^{\mathrm{E}} = 2.1611\times10^{-2}$.

Taking as reference the constant diffusion case (first entry), we can see that increasing the diffusion around the maximum (third entry) has the effect to give the greatest acceleration, *i.e.* greatest eigenvalues, compared to the others. One can qualitatively imagine that increasing the diffusion (and so, lowering friction) around the maximum has the same effect of directly lowering the energy barrier, by the way, we remark that further insights would be only speculative at this point.

Finally, in Figure 5 (panel a) we report the relaxing profile till the equilibrium state, built using 101 DVR points at each time propagation step with constant diffusion and a gaussian initial distribution centered at $x = 4.5$ and with standard deviation $\sigma = 0.05$. It can be noted the initial rapid broadening of the profile $p(x,t)$ due to the fast "fluctuation" processes inside the potential well; these are related to large eigenvalues. As time progresses, the other deeper minimum starts to become populated; this slow population movement between wells is a low activated process related to λ_1. Finally the profile reaches the equilibrium distribution, that matches perfectly the analytic one (see panel b).

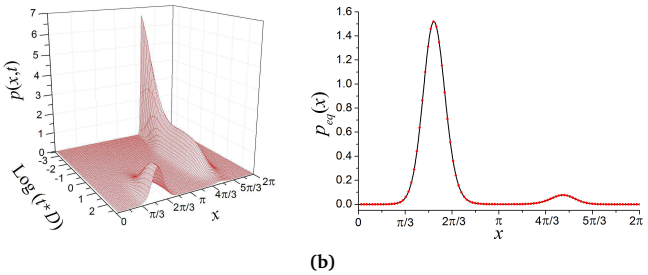

Fig. 5 (a) Surface plot for the relaxation profile $p(x,t)$ of the non-symmetric diffusive problem eqn (34) with constant diffusion and an initial gaussian distribution centered at $x = 4.5$ and $\sigma = 0.05$. The profile is calculated using 101 DVR grid points at each step of time propagation; this last is expressed in decimal logarithm units. (b) Analytic equilibrium distribution $p_{eq}(x)$ for the non-symmetric problem (black line), and extrapolated from relaxation profile (red dots).

3.3 A chemical case-study

As a final example, in order to show the applicability of DVR method to case-studies of chemical interest we consider here the specific case of conformational dynamics of *n*-butane and three dihaloethanes, in particular 1-chloro-2-fluoroethane, 1-bromo-2-fluoroethane, 1-bromo-2-chloroethane (from now on respectively abbreviated as CFE, BFE, BCE). We treat the dynamic as a diffusive motion upon the torsion angle γ of the central C–C bond, taken as the only variable for this problem. For each molecule we solve the Smoluchowski equation using DVR method (as seen before) and we calculate the rate constants for *gauche* $\longleftrightarrow$ *trans* transitions given in diffusion coefficient units.

The internal dynamic is regulated by the conformational energetics that in this case is represented by the torsion potential $V(\gamma)$, generally different for each molecule and by the friction, of viscous nature, that damps the motion. With regard to the friction, that determines the torsion diffusion coefficient, here we shall assume a constant diffusion D. This approximation is valid till we have small molecules in which the two external rotating groups don't have big size. As seen before, as long as D will not have a specific value, it will be only a scaling factor.
The torsion potential for the considered molecules is expressed as

$$V(\gamma) = \alpha_1 \cos\gamma + \alpha_2 \cos 2\gamma + \alpha_3 \cos 3\gamma \qquad (37)$$

a tristable potential, where each well corresponds to a particular molecule conformation, namely the two equivalent *gauche* and the *trans* (from now on respectively abbreviated as g_+, g_- and t); see Figure 6, where the profiles has been shifted to the origin. The potential parameters α_i are taken from ref.[24] for *n*-butane and ref.[25] for dihaloethanes; they are all reported in Table 4 in k_BT units, where $T = 298$ K.

In Table 4 we also report the first three converged eigenvalues calculated with the DVR method (the convergence is reached using only 41 grid points), given in diffusion coefficient units and shown up to five significant figures, for the examined molecules.

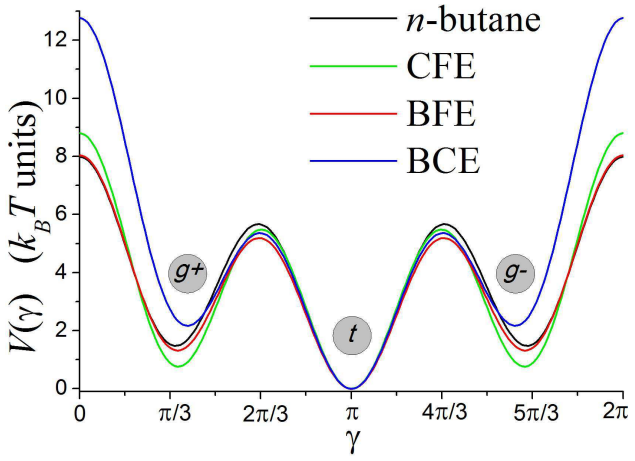

Fig. 6 Plot of the torsion potential $V(\gamma)$, eqn (37), for the examined molecules; profiles are shifted with respect to the origin in order to emphasize the energy barriers involved. The parameters employed to build the profiles are reported in Table 4.

Table 4 Potential parameters (in k_BT units, $T = 298$ K) used for the potential profiles $V(\gamma)$ shown in Figure 6, taken from refs.[24,25] and first three converged eigenvalues given in diffusion coefficient units calculated with DVR method and shown up to five significant figures.

Molecule	α_1	α_2	α_3	λ_1^{DVR}	λ_2^{DVR}	λ_3^{DVR}
n-butane	1.285	0.266	2.708	0.060936	0.073656	15.508
CFE	1.402	0.811	2.997	0.035881	0.062864	16.585
BFE	1.419	0.481	2.601	0.073566	0.10030	14.379
BCE	3.377	1.562	3.006	0.13863	0.17044	15.306

These eigenvalues have the same values of the ones obtained using OR method with a Fourier basis, for which the matrix elements of the diffusion operator are once again analytical.
It can be readily noticed the presence of two lowest eigenvalues λ_1^{DVR} and λ_2^{DVR} related (in a not straightforward way) to slow "jump" processes and clearly separated by λ_3^{DVR} by two/three orders of magnitude. In all these cases the jump processes are four (the direct transition $g_+ \to g_-$ is kinetically forbidden because of the too high energy barrier involved, and here it will not be considered), even if only two are distinguished, namely $t \to g_\pm$ and $g_\pm \to t$, due to the impossibility to discriminate between g_+ and g_-.

Now the problem is how to relate these two lowest eigenvalues with the rate constants $k_{t\to g_\pm}$ and $k_{g_\pm\to t}$ associated to the "jump" transitions between potential wells. For the chemist used to think in terms of activated processes, indeed, these rate constants are precisely the ones to assume relevance and to constitute phenomenological parameters to be determined from experimental data (or from molecular dynamics simulation of these systems). In phenomenological terms, the transitions between the two *gauche* and the *trans* conformation are described adopting a first order kinetic scheme for the *site populations* evolution. By generic *n*-th "site" we mean the "potential well" inside which there is the *n*-th minimum of the potential profile ($n \equiv t, g_\pm$ in our case); the population of this site is naturally defined integrating the nonequilibrium distribution $p(\gamma,t)$ inside the site domain delimited by the neighbours maxima γ_{n-} and γ_{n+}

$$P_n(t) := \int_{\gamma_{n-}}^{\gamma_{n+}} d\gamma\, p(\gamma,t) \tag{38}$$

in particular, the equilibrium populations are given by

$$P_{eq,n} = \int_{\gamma_{n-}}^{\gamma_{n+}} d\gamma\, p_{eq}(\gamma) \tag{39}$$

The kinetic model regulates the relaxation $P_n(t) \to P_{eq,n}$ starting from generic initial conditions. As anticipated before, for our specific case we adopt the following scheme based on four elementary steps (two by two one the inverse of the other one)

$$\begin{aligned} g_+ &\xrightarrow{k_{g_+\to t}} t \\ t &\xrightarrow{k_{t\to g_+}} g_+ \\ g_- &\xrightarrow{k_{g_-\to t}} t \\ t &\xrightarrow{k_{t\to g_-}} g_- \end{aligned} \tag{40}$$

with $k_{g_+\to t} = k_{g_-\to t}$ and $k_{t\to g_+} = k_{t\to g_-}$ since the symmetry of the potential and considering the principle of microscopic reversibility

$$k_{g_\pm\to t}\, P_{eq,g_\pm} = k_{t\to g_\pm}\, P_{eq,t} \tag{41}$$

in order to guarantee the reaching of the correct equilibrium state.

The crucial point is to find a meeting point between the discretized description (kinetic approach for the transitions between the "sites") and the continuous one (diffusive model for γ). Intuitively the two descriptions are interfaced if a neat separation between the time scales of fast processes (fluctuations inside the wells) and slow processes exists (jumps between wells).
This problem has been formally faced by Moro and Nordio[26,27] using "localized site functions" and since it falls outside the main purpose of this work, here we shall give directly the final result for our cases, namely

$$\begin{aligned} k_{t\to g_\pm} &= \lambda_1 \frac{P_{eq,g_\pm}}{P_{eq,t}} \\ k_{t\to g_\pm} &= \lambda_2 P_{eq,g_\pm} \end{aligned} \tag{42}$$

The two values of $k_{t\to g_\pm}$ would be certainly different, but it can be shown that their difference decrease as the barriers between minima get increased. Consequently the best estimate that we can produce is the arithmetic average of the two rate values

$$k_{t\to g_\pm} = \frac{1}{2}\left(\lambda_1 \frac{P_{eq,g_\pm}}{P_{eq,t}} + \lambda_2 P_{eq,g_\pm}\right) \tag{43}$$

while the rate constant for the back transitions $k_{g_\pm\to t}$ is calculated using microscopic reversibility, eqn (41).
In Table 5 we report the equilibrium populations calculated by numerical integration of eqn (39) and the rate constants given in diffusion coefficient units for the examined molecules, calculated with eqns (41,43) and using $\lambda_1^{\mathrm{DVR}}, \lambda_2^{\mathrm{DVR}}$ reported in Table 4.

Table 5 Equilibrium populations calculated by numerical integration of eqn (39) and rate constants given in diffusion coefficient units calculated with eqns (41,43), using $\lambda_1^{\mathrm{DVR}}, \lambda_2^{\mathrm{DVR}}$ reported in Table 4.

Molecule	$P_{eq,t}$ [a]	$P_{eq,g_\pm}$ [a]	$k_{t\to g_\pm}$	$k_{g_\pm\to t}$
n-butane	0.682	0.159	0.0130	0.0556
CFE	0.529	0.235	0.0154	0.0346
BFE	0.615	0.174	0.0186	0.0694
BCE	0.818	0.0911	0.0155	0.139

[a] Populations are normalized, in fact $P_{eq,t} + 2P_{eq,g_\pm} = 1$.

4 Conclusions

We have presented in this work how to setup a reliable framework to solve the monodimensional Smoluchowski equation making use of sinc-DVR methods in conjunction with product approximation. We have demonstrated the efficiency of the approach calculating the eigenvalues of the diffusion operator for some simple and familiar test-cases and reaching convergence with the use of few grid points. The reliability of the results has been assessed through the comparison with a simple finite difference scheme, which has shown in some cases much poorer performances with respect to DVR. Another strength point of the DVR pseudospectral method is its simplicity, especially concerning code implementation.

We really believe that both the difficulties encountered with a simple FD scheme, where the convergence is reached more slowly, or orthonormal representation, where analytic matrix elements are not always available, can effectively be overcame by use of a discrete variable representation coupled with product approximation. Moreover, there are very encouraging perspectives concerning the application of this approach to multidimensional problems (where FD becomes often unfeasible), or more complicated Smoluchowski equations that contain other coordinate dependent terms, *e.g.* a reactive term.

Indeed, in multidimensional problems if the diffusion operator has no mixed second derivatives and if a direct product basis is used for the multidimensional system, the basis for each dimension may be separately transformed to the DVR. The resulting DVR matrix for the diffusion operator will be very sparse[5], simplifying and speeding-up its construction and diagonalization. For more complicated diffusion operators, direct product DVR's in conjunction with product approximation are still highly advantageous leading to straightforward simplifications of the matrix representation of the operator[7,11]. Despite the simplicity of these approaches, it is difficult to predict *a priori* the numerical limit of the same. We believe that a repeated use of product approximation will spoil the eigenvalues convergence; by the way, further insights and work has to be done in order to validate this assumption.

As a final consideration, in order to have a proper modelization of the diffusion function $D(x)$ it is necessary to construct reliable hydrodynamical models, a task that it not always straightforward. However, even if this argument was not central to this work, we mention that our future investigations would cover also these important aspects, starting from the past works that has been done in this field[22,28,29], in order to have sound variable diffusion functions, even for multidimensional problems (where diffusion becomes a tensor). Once reliable informations upon diffusion are achieved (in conjunction with the energetics of the system under study) one can complete the picture of the diffusive problem, *e.g.* calculating absolute kinetic constants for the molecules examined in Section 3.3 and comparing them with their estimates available in literature.

Acknowledgement

The authors are very grateful to Dimitrios Skouteris (Scuola Normale Superiore) and Diego Frezzato (University of Padova) for useful and fruitful discussions.

Appendix A - General theory of DVR

The theory that underlies DVR finds its mathematical roots upon the theory of Gaussian quadratures which is in turn intimately linked with the theory of orthogonal polynomials, even if it is possible to construct DVR starting from other orthogonal functions, like the sinc-DVR built from the Fourier basis (see below). Consider a set of polynomials $\rho(x)$ orthogonal with respect to a weight function $w(x) \geq 0$ on the interval $[a,b]$ (where a and b may be $\pm\infty$), with a scalar product defined as:

$$\langle \rho_m | \rho_n \rangle = \int_a^b dx\, w(x)\, \rho_m(x)\, \rho_n(x) = \delta_{mn} \tag{44}$$

The integral

$$I[f] = \int_a^b dx\, w(x)\, f(x) \tag{45}$$

may be written as

$$I[f] = \langle \rho_0 | f \rangle \tag{46}$$

with $\rho_0(x) \equiv 1$. An N-point quadrature approximation to the integral is defined by N points $\{x_1, \ldots, x_N\}$ and weights $\{w_1, \ldots, w_N\}$

$$I[f] = \sum_{i=1}^{N} w_i\, f(x_i) \tag{47}$$

and is exact for the first $2N$ orthogonal polynomials $\rho_0, \ldots, \rho_{2N-1}$. This is possible since there are precisely $2N$ parameters (x_i, w_i) that may be chosen. We want to eliminate the weight function from the definition of the scalar product, and in order to do so we introduce the functions

$$\phi_n(x) = \sqrt{w(x)}\, \rho_{n-1}(x), \quad n = 1, \ldots, N \tag{48}$$

where we have absorbed the square root of the weight function. Then the orthonormality relations are given exactly by the quadrature

$$\langle \phi_m | \phi_n \rangle = \int_a^b dx\, \phi_m^*(x)\, \phi_n(x) = \delta_{mn} = \sum_{i=1}^{N} \frac{w_i}{w(x_i)}\, \phi_m^*(x_i) \phi_n(x_i) \tag{49}$$

and since the Gaussian quadrature is exact for polynomials of degree $2N-1$ we also find that the quadrature approximations of the matrix elements

$$X_{mn} = \langle \phi_m | x | \phi_n \rangle = \sum_{i=1}^{N} \frac{w_i}{w(x_i)}\, \phi_m^*(x_i) x_i\, \phi_n(x_i) \tag{50}$$

are exact. If now we define the elements of the transformation matrix $\mathbf{U}$ as

$$U_{im} = \sqrt{\frac{w_i}{w(x_i)}}\,\phi_m(x_i) \tag{51}$$

we can easily see that $\mathbf{U}$ is a unitary matrix

$$(\mathbf{U}^\dagger\mathbf{U})_{mn} = \sum_{i=1}^{N} U^*_{im}U_{in} = \sum_{i=1}^{N} \frac{w_i}{w(x_i)}\,\phi^*_m(x_i)\,\phi_n(x_i) = \delta_{mn} \tag{52}$$

and that eqn (50) can be rewritten in matrix form as

$$\mathbf{X} = \mathbf{U}^\dagger\,\mathbf{X}^{\mathrm{DVR}}\,\mathbf{U} \tag{53}$$

where $\mathbf{X}^{\mathrm{DVR}}$ is a diagonal matrix of DVR points $\{x_i\}$. Since $\mathbf{U}$ is unitary, eqn (53) also states that DVR points can be found diagonalizing the coordinate matrix $\mathbf{X}$:

$$\mathbf{U}\,\mathbf{X}\,\mathbf{U}^\dagger = \mathbf{X}^{\mathrm{DVR}} \tag{54}$$

Thus the Gaussian quadrature points are the DVR points and $\mathbf{U}$ is the transformation between the so called Finite Basis Representation (FBR) and DVR. The idea of a DVR, is to apply the unitary transformation to the basis $\{\phi_1(x),\ldots,\phi_n(x)\}$

$$\theta_i(x) = \sum_{i=1}^{N} U^*_{im}\phi_m(x) \tag{55}$$

in order to have basis functions localized on grid points x_i

$$\theta_i(x_j) = \sum_{i=1}^{N} U^*_{im}\phi_m(x_j) = \sum_{i=1}^{N} \sqrt{\frac{w(x_j)}{w_j}}\,U^*_{im}U_{jm} = \sqrt{\frac{w(x_j)}{w_j}}\,\delta_{ij} \tag{56}$$

Thus, any multiplicative operator (*e.g.* $G(x)$ here) will be diagonal in this basis if quadrature approximation is used

$$(\mathbf{G}^{\mathrm{DVR}})_{jk} = \langle\theta_j|G(x)|\theta_k\rangle = \sum_{i=1}^{N} \frac{w_i}{w(x_i)}\,\theta^*_j(x_i)\,G(x_i)\,\theta_k(x_i) = G(x_i)\,\delta_{jk} \tag{57}$$

It is clear that different kind of operators, such as derivative operators ($\frac{d}{dx}, \frac{d^2}{dx^2},\ldots$), will not be diagonal in a DVR and it will be necessary to find their representation in the chosen DVR basis, ($\mathbf{D}^{\mathrm{DVR}}$ in the text).

sinc-DVR

This DVR is constructed starting from Fourier basis; following Tannor[10] we show the similarity between this DVR and the ones built from a set of orthogonal polynomials. We consider the band limited Fourier orthogonal basis functions, *i.e.* functions that have no component of $|k|$ beyond K, and in the infinite x space range the basis functions are of the form

$$\phi_k(x) = \frac{e^{ikx}}{\sqrt{2\pi}}\,, \quad -K \le k \le K\,, \quad -\infty < x < \infty \tag{58}$$

The orthogonality relation is now expressed as

$$\langle\phi_{k'}|\phi_k\rangle = \int_{-\infty}^{\infty} dx\,\phi^*_{k'}(x)\,\phi_k(x) = \int_{-\infty}^{\infty} dx\,\frac{e^{i(k-k')x}}{2\pi} = \delta(k-k')$$

$$= \sum_{j=-\infty}^{\infty} \Delta x\,\phi^*_{k'}(x_j)\,\phi_k(x_j) = \sum_{j=-\infty}^{\infty} \Phi^*_{k'}(x_j)\,\Phi_k(x_j) \tag{59}$$

Taking $\Delta x = \frac{2\pi}{2K}$, $x_j = j\Delta x = \frac{j\pi}{K}$, the basis orthogonality relation is exact for

$$\Phi_k(x_j) = \frac{e^{ikx_j}}{\sqrt{2K}} \tag{60}$$

In order to construct the DVR basis we perform a Fourier transform on the basis set, obtaining a basis that is complete for all band limited functions

$$\int_{-K}^{K} dk\,\Phi^*_k(x_j)\,\phi_k(x) = \theta_j(x) = \int_{-K}^{K} dk\,\frac{e^{-ikx_j}}{\sqrt{2K}}\,\frac{e^{ikx}}{\sqrt{2\pi}}$$

$$= \frac{\sin(K(x-x_j))}{\sqrt{\pi K}(x-x_j)} = \sqrt{\frac{K}{\pi}}\,\mathrm{sinc}[K(x-x_j)] \tag{61}$$

It is readily seen that each sinc function is centered on a different grid point for a uniform grid, $x_j = j\Delta x$, with $\Delta x = \frac{\pi}{K}$; cf. eqn (16) in the text. Another simple derivation of this sinc-DVR starting with particle-in-a-box basis eqn (17) is presented in Appendix A of ref.[5].

Appendix B - Finite difference scheme

The monodimensional Smoluchowski equation (eqn (5) in the text) can be compacted introducing the probability flux $J(x,t)$ as

$$\frac{\partial}{\partial t}\,p(x,t) = -\frac{\partial J(x,t)}{\partial x} \tag{62}$$

with

$$\frac{\partial J(x,t)}{\partial x} = -D(x)\,p_{eq}(x)\,\frac{\partial}{\partial x}\,p^{-1}_{eq}(x)\,p(x,t) \tag{63}$$

Given that x varies between the endpoints $x_{\min}$ and $x_{\max}$, we partition the domain $[x_{\min},x_{\max}]$ into N intervals (here $N \equiv N_{\mathrm{points}}$ in the text), each one labeled by the central point x_n belonging to the same interval and by its endpoints, respectively $x^-_n \equiv x^+_{n-1}$ (left) and $x^+_n \equiv x^-_{n+1}$ (right). The intervals length is chosen to be the same; *i.e.* $\Delta x = \frac{x_{\min}-x_{\max}}{N}$. Eqn (62) evaluated in the generic point x_n can be approximated as incremental ratio

$$\frac{\partial}{\partial t}\,p(x_n,t) = -\frac{\partial J(x_n,t)}{\partial x} \simeq -\frac{J(x^+_n,t)-J(x^-_n,t)}{\Delta x} \tag{64}$$

It is possible to set out the fluxes evaluated at the n-th interval endpoints using eqn (63) and approximating again the derivative as incremental ratio. Collecting the factors and introducing the column vector $\mathbf{P}(t)$ with elements $P_n(t) = p(x_n,t)$ $(n = 1,2,\ldots,N)$ one obtains the following matrix relation

$$\dot{\mathbf{P}}(t) = -\mathbf{\Gamma}(t)\,\mathbf{P}(t) \tag{65}$$

where $\mathbf{\Gamma}(t)$ is a tridiagonal matrix with elements

$$\Gamma_{n,m}(t) = \begin{cases} \delta_{m,n} \frac{p_{eq}^{-1}(x_n)}{\Delta x^2} [D(x_n^+) p_{eq}(x_n^+) + D(x_n^-) p_{eq}(x_n^-)] \\ -\delta_{m,n+1} \frac{p_{eq}^{-1}(x_{n+1})}{\Delta x^2} D(x_n^+) p_{eq}(x_n^+) \\ -\delta_{m,n-1} \frac{p_{eq}^{-1}(x_{n-1})}{\Delta x^2} D(x_n^-) p_{eq}(x_n^-) \end{cases} \quad (66)$$

To complete the procedure it is necessary to set the proper boundary conditions on fluxes in correspondence with the domain endpoints $x_{\min}, x_{\max} \equiv x_1^-, x_N^+$. For reflective boundary conditions, the flux at the endpoints must vanish

$$J(x_1^-, t) = 0 \quad \text{and} \quad J(x_N^+, t) = 0 \quad (67)$$

at any t. This implies that

$$\begin{aligned} \Gamma_{1,1}(t) &= \frac{p_{eq}^{-1}(x_1)}{\Delta x^2} D(x_1^+) p_{eq}(x_1^+) \\ \Gamma_{N,N}(t) &= \frac{p_{eq}^{-1}(x_N)}{\Delta x^2} D(x_N^-) p_{eq}(x_N^-) \end{aligned} \quad (68)$$

On the other hand, for periodic boundary conditions, it must be

$$J(x_1^-, t) = J(x_N^+, t) \quad (69)$$

at any t. This implies that

$$\begin{aligned} \Gamma_{1,1}(t) &= \frac{p_{eq}^{-1}(x_1)}{\Delta x^2} [D(x_1^+) p_{eq}(x_1^+) + D(x_1^-) p_{eq}(x_1^-)] \\ \Gamma_{1,N}(t) &= -\frac{p_{eq}^{-1}(x_N)}{\Delta x^2} D(x_1^-) p_{eq}(x_1^-) \\ \Gamma_{N,1}(t) &= -\frac{p_{eq}^{-1}(x_1)}{\Delta x^2} D(x_N^+) p_{eq}(x_N^+) \\ \Gamma_{N,N}(t) &= \frac{p_{eq}^{-1}(x_N)}{\Delta x^2} [D(x_N^+) p_{eq}(x_N^+) + D(x_N^-) p_{eq}(x_N^-)] \end{aligned} \quad (70)$$

Finally the eigenvalues λ^{FD}'s are found by diagonalizing $\mathbf{\Gamma}$.

References

1 A. Pedone, E. Gambuzzi, V. Barone, S. Bonacchi, D. Genovese, E. Rampazzo, L. Prodi, M. Montalti. Understanding the photophysical properties of coumarin-based Pluronic-silica (PluS) nanoparticles by means of time-resolved emission spectroscopy and accurate TDDFT/stochastic calculations. *Phys. Chem. Chem. Phys.* **2013**, *15*, 12360–12372.

2 C. W. Gardiner, *Handbook of Stochastic Methods: For Physics, Chemistry and the Natural Sciences*, of *Springer series in synergetics*, Springer, **1985**.

3 P. Banushkina, M. Meuwly. Hierarchical Numerical Solution of Smoluchowski Equations with Rough Potentials. *J. Chem. Theory Comput.* **2005**, *1*, 208–214.

4 J. Dunkel, W. Ebeling, L. Schimansky-Geier, P. Hänggi. Kramers problem in evolutionary strategies. *Phys. Rev. E* **2003**, *67*, 061118.

5 D. T. Colbert, W. H. Miller. A novel discrete variable representation for quantum mechanical reactive scattering via the S-matrix Kohn method. *J. Chem. Phys.* **1992**, *96*, 1982–1991.

6 G. H. Gardenier, M. A. Johnson, A. B. McCoy. Spectroscopic Study of the Ion-Radical H-Bond in $H_4O_2^+$. *J. Phys. Chem. A* **2009**, *113*, 4772–4779.

7 H. Wei, T. Carrington. Discrete variable representations of complicated kinetic energy operators. *J. Chem. Phys.* **1994**, *101*, 1343–1360.

8 G. C. Groenenboom, D. T. Colbert. Combining the discrete variable representation with the S-matrix Kohn method for quantum reactive scattering. *J. Chem. Phys.* **1993**, *99*, 9681–9696.

9 D. Luckhaus. 6D vibrational quantum dynamics: Generalized coordinate discrete variable representation and (a)diabatic contraction. *J. Chem. Phys.* **2000**, *113*, 1329–1347.

10 D. J. Tannor, *Introduction to Quantum Mechanics: A Time-dependent Perspective*, University Science Books, **2007**.

11 J. C. Light, T. Carrington, *Discrete-Variable Representations and their Utilization*, *Vol. 114*, John Wiley & Sons, Inc., **2007**, pp. 263–310.

12 V. Szalay. Discrete variable representations of differential operators. *J. Chem. Phys.* **1993**, *99*, 1978–1984.

13 J. C. Light, I. P. Hamilton, J. V. Lill. Generalized discrete variable approximation in quantum mechanics. *J. Chem. Phys.* **1985**, *82*, 1400–1409.

14 Z. Bačić, J. C. Light. Theoretical Methods for Rovibrational States of Floppy Molecules. *Annu. Rev. Phys. Chem.* **1989**, *40*, 469–498.

15 G. E. Uhlenbeck, L. S. Ornstein. On the Theory of the Brownian Motion. *Phys. Rev.* **1930**, *36*, 823–841.

16 H. Risken, *The Fokker-Planck Equation: Methods of Solution and Applications*, of *Lecture Notes in Mathematics*, Springer Berlin Heidelberg, **1996**.

17 The diffusion operator eigenfunctions in this case are simply given by Hermite polynomials.

18 P. Hänggi, P. Talkner, M. Borkovec. Reaction-rate theory: fifty years after Kramers. *Rev. Mod. Phys.* **1990**, *62*, 251–341.

19 N. G. Van Kampen, *Stochastic Processes in Physics and Chemistry*, of *North-Holland Personal Library*, Elsevier Science, **2011**.

20 H. A. Kramers. Brownian motion in a field of force and the diffusion model of chemical reactions. *Physica* **1940**, *7*, 284–304.

21 O. Edholm, O. Leimar. The accuracy of Kramers' theory of chemical kinetics. *Physica* **1979**, *98A*, 313–324.

22 V. Barone, M. Zerbetto, A. Polimeno. Hydrodynamic modeling of diffusion tensor properties of flexible molecules. *J. Comput. Chem.* **2009**, *30*, 2–13.

23 R. Zwanzig, *Nonequilibrium Statistical Mechanics*, Oxford University Press, USA, **2001**.

24 W. L. Jorgensen, J. D. Madura, C. J. Swenson. Optimized intermolecular potential functions for liquid hydrocarbons. *J. Am. Chem. Soc.* **1984**, *106*, 6638–6646.

25 J. Huang, K. Hedberg. Conformational analysis. 14. The di-

haloethanes $ClCH_2CH_2F$, $BrCH_2CH_2F$, and $BrCH_2CH_2Cl$. Investigations of the molecular structures, rotameric compositions, anti and gauche energy and entropy differences, and barriers hindering internal rotation by gas-phase electron diffraction augmented by rotational constants and ab initio calculation. *J. Am. Chem. Soc.* **1990**, *112*, 2070–2075.

26 G. Moro, P. L. Nordio. Diffusive and jump description of hindered motions. *Mol. Phys.* **1985**, *56*, 255–269.

27 G. Moro, P. L. Nordio. Diffusion between inequivalent sites. *Mol. Phys.* **1986**, *57*, 947–955.

28 A. Ferrarini, G. Moro, P. L. Nordio. Conformational kinetics of aliphatic tails. *Mol. Phys.* **1988**, *63*, 225–247.

29 B. Nigro, D. Di Stefano, A. Rassu, G. J. Moro. Cranklike conformational transitions in polyethylene. *J. Chem. Phys.* **2004**, *121*, 4364–4376.